

INTERNATIONAL SOCIETY FOR SOIL MECHANICS AND GEOTECHNICAL ENGINEERING



This paper was downloaded from the Online Library of the International Society for Soil Mechanics and Geotechnical Engineering (ISSMGE). The library is available here:

<https://www.issmge.org/publications/online-library>

This is an open-access database that archives thousands of papers published under the Auspices of the ISSMGE and maintained by the Innovation and Development Committee of ISSMGE.

The paper was published in the proceedings of the 10th European Conference on Numerical Methods in Geotechnical Engineering and was edited by Lidija Zdravkovic, Stavroula Kontoe, Aikaterini Tsiampousi and David Taborda. The conference was held from June 26th to June 28th 2023 at the Imperial College London, United Kingdom.

To see the complete list of papers in the proceedings visit the link below:

<https://issmge.org/files/NUMGE2023-Preface.pdf>

Large deformation modeling of landslides using stochastic MPM with interdependent variables

G. Ma^{1,2}, M. Rezaia^{1,2}, M. Mousavi Nezhad¹

¹*School of Engineering, University of Warwick, Coventry, United Kingdom*

²*Faculty of Geosciences and Environmental Engineering, Southwest Jiaotong University, Chengdu, China*

ABSTRACT: In this study, a stochastic modeling method considering the interdependent heterogeneities of soil deposits is proposed to reduce the uncertainties in predicting landslides' post-failure deformations. The proposed method is implemented in the context of a generalised interpolation material point method (GIMP) to investigate large-deformation processes after landslide failure. The cross-correlated random fields are characterised and represented for multiple interdependent properties with cross-correlation for randomly distributed soil mass. A Monte-Carlo simulation approach is adopted, and a series of realisations of bivariate random fields are generated and used as input data for GIMP analysis. The results indicate that the proposed method is capable of reproducing post-failure behavior of heterogeneous landslides considering frictional features. It is found that the mean value of final runout distance in heterogeneous landslides is higher than that of the deterministic value obtained from a homogeneous analysis. Based on the distributions of calculated runout distances for heterogeneous analyses, in over 50% of cases larger runout distances are obtained than those from the deterministic analysis. Hence, it is observed that the inherent interdependent heterogeneity would notably increase the variability and uncertainty of post-failure behavior of landslides, and as such its consideration is essential for reliable risk assessment against these geohazards.

Keywords: Landslides; Heterogeneity; Cross-correlated random fields; Large deformation; Hazard management

1 INTRODUCTION

Landslides occur every year in mountainous areas in the world. Soil properties with interdependencies exhibit considerable spatial variability in strength, which has profound impacts on instability of landslides and runout motions (Zhu et al., 2019; Ma et al., 2022a). Diverse failure consequences can be observed in a varying soil slope consisting of weak materials (e.g., weak intercalation layer) because the failure surface tends to seek out the weakest path. Due to extensive runout motions of landslides during the post-failure stage, substantial destruction can be observed on nearby structures (Yin et al., 2016), which leads to severe threat and significant damages to human life and properties (Ma et al., 2018). Studies of post-failure behaviors in soil slopes are very complicated due to large deformations and interdependencies in spatially varying shear strengths of soil. Thus, it is necessary to propose a reliable prediction model to assess the probable post-failure consequences and potential impacts.

Material point method (MPM), a particle-based method, has been widely adopted to simulate large strain geotechnical problems (Sulsky et al., 1994). However, in previous studies, the materials were primarily assumed to be simply homogeneous, and the geomaterials' responses have been modeled deterministically using constant values of soil parameters. Recently,

Remmerswaal et al. (2021) utilized the random MPM combined with Monte-Carlo simulations (MCS) to investigate residual dyke resistance after initial failure. Ma et al. (2022b) adopted stochastic MPM incorporating univariate random fields for quantifying landslide influence zone. However, the models only considered one shear strength parameter (e.g., undrained shear strength) as a random variable, and as such their models are unable to deal with deposits with frictional characteristics. This paper employed a new probabilistic modeling method termed stochastic material point method (SMPM) for estimating post-failure behavior of landslides with interdependent geotechnical variables in cohesive-frictional soil, where the cross-correlated bivariate random fields (interdependent cohesion and friction angle parameters) are incorporated into the generalized interpolation MPM (GIMP) through an MCS algorithm. This work will provide a new insight for assessing the potential impact of a slope stability hazard.

2 STOCHASTIC MATERIAL POINT METHOD

2.1 Cross-correlated random fields

Random field (RF) modeling has been widely used to mathematically characterize the spatial variability of

shear strength in soils. In a RF, an important measure of the variability is the autocorrelation distance, which may not be constant for different directions in a soil mass. The spatial variability of soils' shear strength could entail autocorrelation distance ranging from less than 1 m to tens of meters along different directions. In this paper, a squared exponential autocorrelation function (ACF) is used to characterize spatial variability of soil parameters (Ma et al., 2022a). The correlation coefficient $\rho(\tau_x, \tau_y)$ and scale of fluctuation θ_ϕ are given as

$$\rho(\tau_x, \tau_y) = \exp\left[-\frac{\sqrt{\tau_x^2 + \tau_y^2}}{\theta}\right] \quad (1)$$

$$\theta_\phi = \theta_1 = \theta_2 \quad (2)$$

where τ_x and τ_y are the relative distances between any two points in horizontal and vertical directions, respectively; θ_1 and θ_2 are the scales of fluctuation in principal directions.

In this work, Cholesky matrix decomposition method (CMD) is adopted to generate RFs because of its wide application in geotechnical analysis (Ma et al., 2022b). Once the ACF is determined, the domain Ω can be discretized into n elements of the RF with the centroid coordinates of the elements. The autocorrelation matrix $\mathbf{C}_{n \times n}$, representing the spatial variability of the soil properties. Subsequently, the $\mathbf{C}_{n \times n}$ can be decomposed by Cholesky matrix decomposition method into the product of a lower triangular matrix \mathbf{L} and a conjugate transpose \mathbf{L}^T . In soil mass, cohesion, c , and friction angle, ϕ , are the significant factors influencing slope failure, and they are found to be negatively cross-correlated with each other with a Pearson cross-correlation coefficient $\rho_{c,\phi}$. A cross-correlation matrix $\mathbf{R}_{2 \times 2}$ between c and ϕ can be formed as

$$\mathbf{R}_{2 \times 2} = \begin{bmatrix} 1 & \rho_{c,\phi} \\ \rho_{c,\phi} & 1 \end{bmatrix} \quad (3)$$

The $\mathbf{R}_{2 \times 2}$ can be decomposed by using Cholesky decomposition techniques to obtain \mathbf{L}_ρ , and the cross-correlated Gaussian RFs can be expressed as

$$\mathbf{X}^{CG} = \mathbf{L}_\rho \cdot \begin{bmatrix} \mathbf{X}_c^{IG} \\ \mathbf{X}_\phi^{IG} \end{bmatrix} = \begin{bmatrix} 1 & 0 \\ \rho_{c,\phi} & \sqrt{1 - \rho_{c,\phi}^2} \end{bmatrix} \cdot \begin{bmatrix} \mathbf{X}_c^{IG} \\ \mathbf{X}_\phi^{IG} \end{bmatrix} \quad (4)$$

In this work, the shear strength parameters (c and ϕ) are consumed as lognormally distributed to avoid negative values, the realization of a cross-correlated lognormal RF can be obtained by exponential function

$$\mathbf{X}^{LN} = \begin{bmatrix} \mathbf{X}_c^{LN} \\ \mathbf{X}_\phi^{LN} \end{bmatrix} = \begin{bmatrix} \exp(\mu_{ln c} + \sigma_{ln c} \cdot \mathbf{X}_c^{CG}) \\ \exp(\mu_{ln \phi} + \sigma_{ln \phi} \cdot \mathbf{X}_\phi^{CG}) \end{bmatrix} \quad (5)$$

where $\mu_{ln c}$ and $\sigma_{ln c}$ are the mean and standard deviation of Gaussian random variable $ln c$, respectively; $\mu_{ln \phi}$ and $\sigma_{ln \phi}$ are the mean and standard deviation of Gaussian random variable $ln \phi$, respectively. The procedure can be repeated N times to obtain N simulations of the cross-correlated RFs that representing interdependent variables in soil mass.

2.2 Material point method

After obtaining cross-correlated RFs, the runout distance of landslides can be captured by MPM analysis. In this paper, the open-source GIMP program named MPM3D from the Computational Dynamics Laboratory of Tsinghua University (Zhang et al., 2016) is adopted for the analysis. The implementation of computational cycle of GIMP can be found in several published literatures (e.g., Li et al., 2020). Meanwhile, as for the time when the stress is updated, the modified update stress last (MUSL) is adopted in this work to provide better computational stability (Nairn, 2003).

As for the soil mass behavior, it is modeled as elastic-perfectly plastic materials with the Mohr-Coulomb failure criterion. It is assumed that the strength properties are significantly degraded in mobilized soil mass during the sliding. The strain-softening behavior induced by increasing deviatoric plastic strain is used (Ma et al., 2022b).

2.3 Implementation

In this work, GIMP is coupled with the cross-correlated RFs under MCS framework. Firstly, an RF mesh is generated for a sampling process. The CMD method is employed, and a computational algorithm is written using PYTHON 3.9 to obtain bivariate cross-correlated RF samples of shear strength parameters over the computational mesh. Then, the samples are mapped onto the material points in the GIMP, in which each particle has a unique value of soil properties (c and ϕ). The transmission process is based on the spatial relationship between material point and RF mesh element (e.g., a position-to-position mapping process), which is similar to the approach used in the random FEM (Huang et al., 2020). Therefore, the sample values of each element in the RF mesh are assigned to the corresponding material points according to their spatial coordinates. It should be noted that each material point carries random values based on the RF, namely, c and ϕ , respectively.

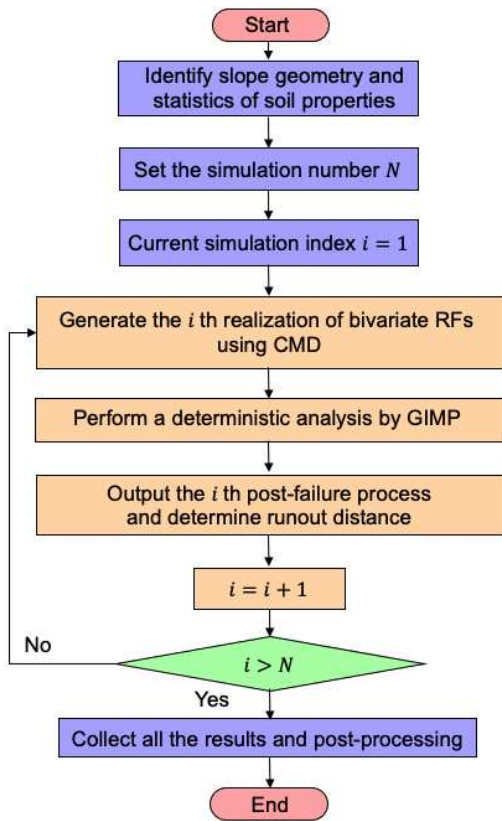


Figure 1. Flowchart of the probabilistic analysis of landslides considering cross-correlated random fields

Figure 1 shows the computational flowchart of the SMPM with the details summarized in the following steps:

1. Identify the input information for probabilistic analysis of post-failure behavior, including slope geometry, statistics of c and φ (i.e., mean, standard deviation, distribution type, ACF, autocorrelation distance) and establish the GIMP deterministic slope model.
2. Set the total number of RFs, N ; the current simulation starts from $i = 1$.
3. Discretize the domain into n elements and extract the centroid coordinates of each element. Based on prescribed statistical information of the soil properties, one isotropic bivariate Gaussian RF is generated and subsequently it is transformed into a non-Gaussian RF $\mathbf{X}_i^{LN}(x, y)$ of c and φ .
4. Determine the runout distance by performing a deterministic GIMP analysis of a landslide with the i -th RF generated in step 3.
5. Update the simulation index, i , and repeat N times. It should be noted that each simulation index i would be updated and checked, if $i > N$, abort the MCS, otherwise continue.

All calculated results (e.g., runout distances) are collected and post-processed to estimate the

corresponding best-fit marginal distribution and statistical characteristics.

3 ILLUSTRATIVE EXAMPLE

An example cohesive-frictional soil slope is considered to show the feasibility of the proposed probabilistic post-failure analysis of landslides. Figure 2 shows the geometry of the slope with 15 m height and a slope gradient of 45° . A mesh with four-noded square elements of size 0.2 m is used, where in each element there are 4 equally spaced material points with a size of 0.1 m. The total number of material points is 10,090. The RF is generated with a cell size equal to material point domain (0.1 m), where the properties of a single cell correspond to one material point. Therefore, as RF cell is 4 times smaller than the smallest scale of fluctuation, the spatial variability is adequately captured. The bottom of the slope is a fixed boundary, both lateral sides are roller type symmetrical boundaries, and the top boundary is free.

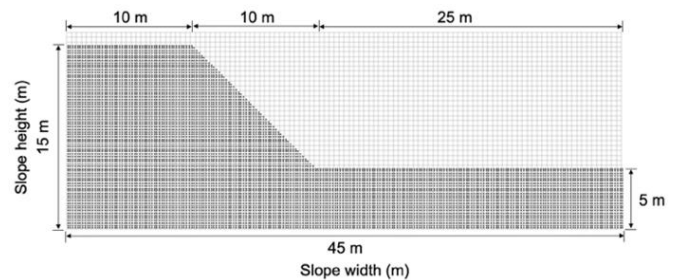


Figure 2. Geometry and material point model for the example slope

As the shear strength of soil deposit is spatially distributed, the c and φ are considered as cross-correlated bivariate RFs. The COV values for c and φ are set as 0.1 according to the typical values summarized (Wu, 2015). For incorporating the dependence relationship between c and φ , a cross-correlation coefficient $\rho_{c,\varphi}$ is set as a typical value with -0.5 . The mean values for c and φ are 20 kPa and 10° , and their autocorrelation distances in horizontal and vertical direction are 20 m and 2 m, respectively. Typical values are assigned to other parameters, i.e., Young's modulus $E = 100$ MPa, Poisson's ratio $\nu = 0.35$, and unit weight $\gamma = 20$ kN/m³, as their contributions on landslide runout distance are not significant. The residual cohesion is set as 10 kPa and residual friction angle is set equal to 5° . The initial *in-situ* stresses are generated using gravitational loading. The total duration for the calculation is 10 s, when soil deposits become stable according to kinematic energy and unbalanced forces of the system (Kafaji, 2013).

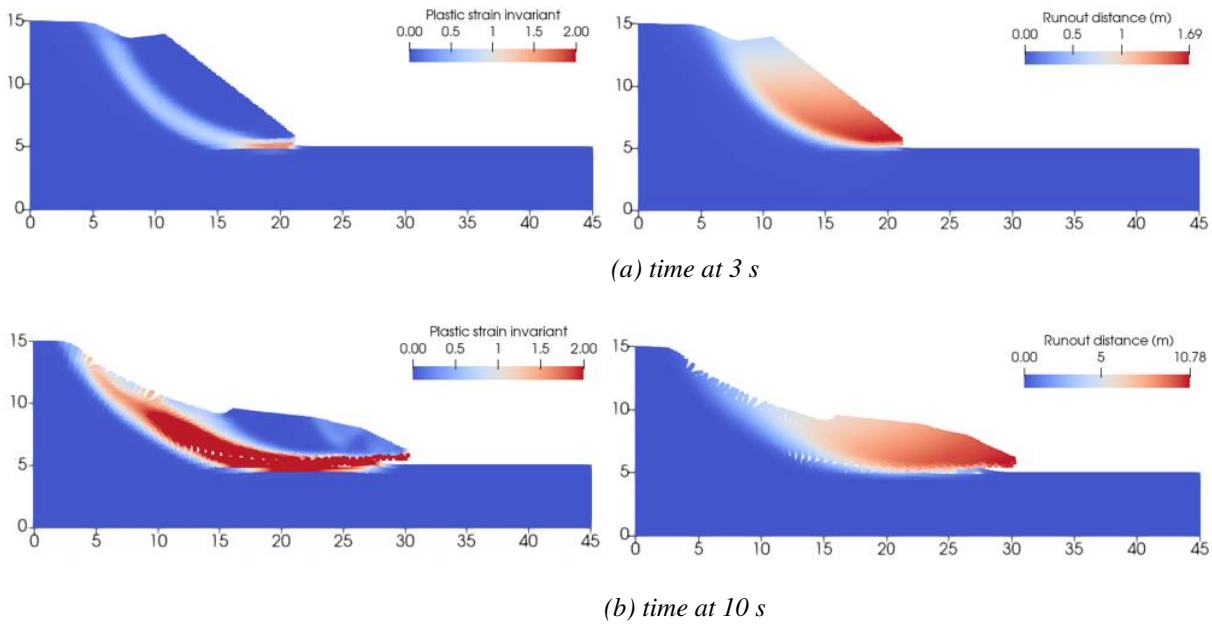


Figure 3. Configurations of landslide by deterministic analysis at critical times

3.1 Deterministic analysis

In the deterministic model, all mechanical parameters are constant and the mean values of c and ϕ are used. Figure 3 shows the runout motions of the landslide computed with the deterministic model. At $t = 3.0$ s, the destruction of the failure block is evident, at this moment the mass slide about 1.7 m away from the initial toe of the slope (Figure 3(a)). At $t = 5$ s, the maximum soil displacement reaches 7.55 m (Figure 3(b)). Then, the sliding mass further moves downward along a fully connected rotational rupture surface and spreads onto the ground. During the post-failure process, a large deformation can be observed, and the landslide is completely deposited at $t = 11.0$ s (Figure 3(c)). For a quantification of the failure consequence, the runout distance with 10.78 m length is obtained from this calculation.

3.2 Stochastic analysis

Stochastic analyses are conducted to quantify the uncertainties of the post-failure behaviors in the hypothetical example. Figure 4 shows a typical RF sample of c and ϕ values in the slope, respectively (randomly selected from the MC samples). Blue color represents relatively weak parts with low c or ϕ values, while red color represents relatively strong sections with high c or ϕ values. Given the negatively correlated coefficients, the increase of one parameter value decreases the other parameter's value.

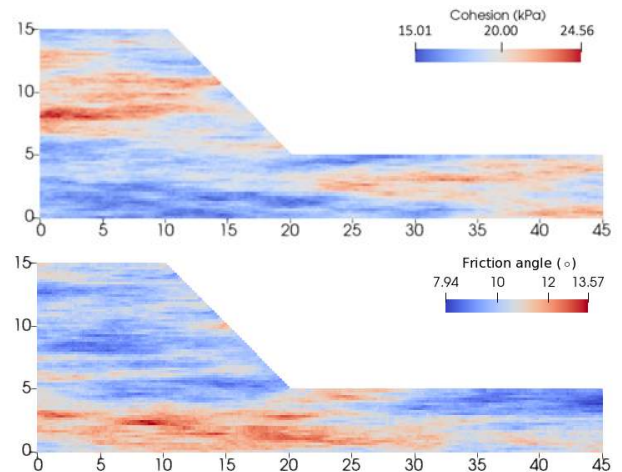


Figure 4. Typical sample of cross-correlated RF of cohesion and friction angle

According to the GIMP simulation, the runout distance of the landslide with the spatially varying soil properties is obtained as 12.14 m (see Figure 5), which is larger than the deterministic analysis with 10.78 m. Additionally, based on the sliding mass of landslides, the sliding volume can be obtained from the mobilized particles of numerical model, in which the particles with a displacement larger than 0.1 m are counted. It is found that there are 2312 mobilized particles and 2522 mobilized particles from the homogeneous model and heterogeneous model, respectively. The corresponding sliding volumes are 462.4 m³ for the heterogeneous model and 504.2 m³ for the homogeneous model, respectively. Therefore, the homogeneous case may underestimate the potential risks from the sliding mass.

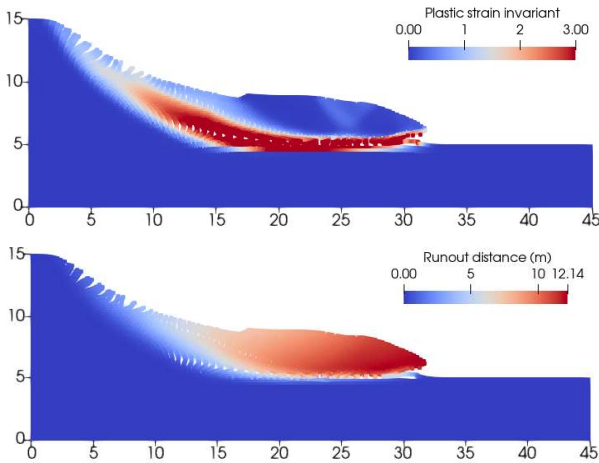


Figure 5. Plastic strain invariant and runout distance of a typical heterogeneous case

It should be noted that the example is analysed with only one set of random distribution and combination of c and ϕ , which means the different RF samples may differ in MC simulations. Consequently, multiple MC simulations are required to capture the range of possible post-failure deformations of the landslide. It is noteworthy that given that the focus of the study is on analyzing post-failure response, only cases where a material points' displacement larger than 1 m occurs are considered as sliding/failure cases. According to the convergence criterion indicated in Section 2, 1000 MCS realizations are performed for this study to confirm stable statistical results and computational efficiency.

In Figure 6, the time-runout distance curves of landslides by MCS through all samples are plotted, which present the calculated runout distance at different times. Different from the homogeneous case, the heterogeneous cases show dramatic uncertainties of runout motions during the sliding time. As for larger runout distance, this is mainly because in some cases the failure paths in the spatially varying soil generally go through relatively weak soil zones, which may lead to an extensive runout distance. While other cases may face strong soil sections through their failure paths and have relatively smaller runout distance. Furthermore, the runout distance of stochastic cases varies substantially at different times, and they distinctly differ from that of the deterministic analysis. At the same time, after 1.0 s, the runout distances of different samples start to differ from one case to another and vary in a relatively wide range of about 3 m at $t=3$ s. For some cases the landslide does not initiate at this moment (i.e., runout distance = 0 m), while at the same time the runout distances of other cases can reach up to about 3 m. Although the runout distance varies from one realization to another, the landslides reach their final equilibrium state in a certain time (between 6.0 s to 8.0 s).

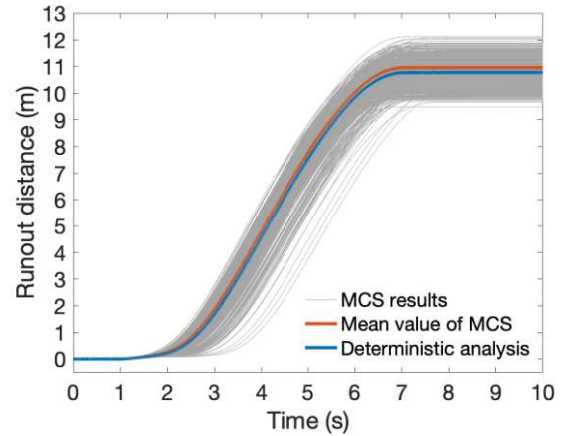


Figure 6. Time-runout distance curves for MCS samples and comparison with the deterministic analysis

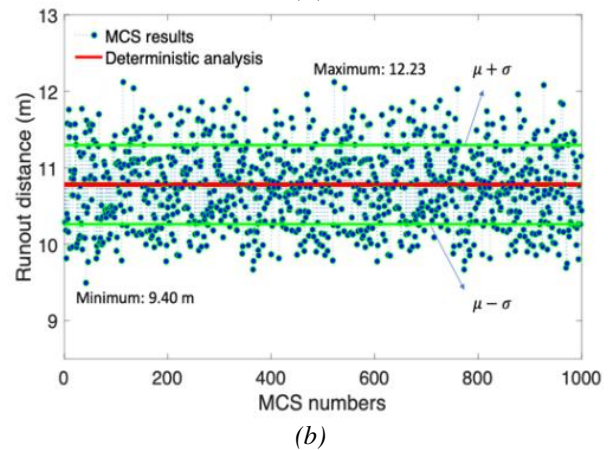
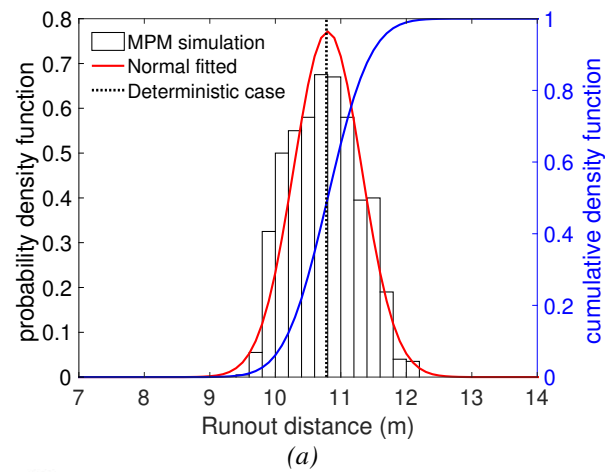


Figure 7. (a) Probability density histogram and (b) scatter plot for the calculated runout distance fitted by a normal distribution

Figure 7(a) shows the probability density histogram for the calculated runout distance from the case with 1000 samples. In this figure, the horizontal coordinate represents the calculated runout distance, the left vertical coordinate represents the probability density function (PDF), and the right coordinate represents the cumulative density function (CDF). The red line is the PDF result fitted by the Normal distribution based on the computed values, and the blue line is the corresponding CDF result. The normal distribution can relatively

describe the predicted runout distances, with an estimated mean value of 10.80 m and standard deviation of 0.51 m. If the deterministic result is considered as a limit of safety, the exceedance probability (runout distance > 10.78 m) is about 52%. Meanwhile, the largest runout distance with 12.23 m and lowest runout distance with 9.49 m obtained from the stochastic analysis notably exceed the limit of safety as shown in Figure 7(b). The results show a notable change in runout distance prediction, between the homogeneous analysis and the heterogeneous analysis.

4 CONCLUSIONS

This study aims to investigate the effect of interdependent heterogeneity in cohesive-frictional soils on the post-failure behavior of landslides using SMPM with cross-correlated bivariate RFs for the strength parameters. The main conclusions obtained from the analyses presented in this work can be summarized as follows:

1. The homogeneous landslide may yield unsafe predictions leading to an underestimation of the runout motions. While a heterogeneous analysis of a slope under landslide conditions would show significant variations in the runout distance.
2. The spatial variability and negative cross-correlation of c and ϕ notably influence the post-failure behavior of landslides. If the deterministic result is considered as a limit of safety, the exceedance probability (runout distance > 10.78 m) is about 52%.
3. The proposed method can be considered as a practical tool to facilitate the evaluation of landslide hazards concerning the impacts of a landslide on neighboring structures.

5 ACKNOWLEDGEMENTS

The financial support by the National Natural Science Foundation of China Project (Contract 52150610492) and SJTU-Warwick Joint Seed Fund are gratefully acknowledged. The first author would like to acknowledge support from Institute of Advanced Study fellowship program, University of Warwick.

6 REFERENCES

- Huang, Y., Li, G., Xiong, M. 2020. Stochastic assessment of slope failure run-out triggered by earthquake ground motion. *Natural Hazards* **101**, 87–102.
- Kafaji, I. K. J. 2013. Formulation of a dynamic material point method (MPM) for geomechanical problems. Ph.D thesis. Germany: University of Stuttgart.
- Li, X., Yan, Q., Zhao, S., Luo, Y., Wu, Y., Wang, D. 2020. Investigation of influence of baffles on landslide debris mobility by 3D material point method. *Landslides* **17**, 1129–1143.
- Ma, G., Rezaia, M., Nezhad, M.M. 2022a. Effects of spatial autocorrelation structure for friction angle on the runout distance in heterogeneous sand collapse. *Transportation Geotechnics* **33**, 100705.
- Ma, G., Rezaia, M., Nezhad, M.M. 2022b. Stochastic assessment of landslide influence zone by material point method and generalized geotechnical random field theory. *International Journal of Geomechanics* **22(4)**, 04022002.
- Ma, G., Hu, X., Yin, Y., Luo, G., Pan, Y. 2018. Failure mechanisms and development of catastrophic rockslides triggered by precipitation and open-pit mining in Emei, Sichuan, China. *Landslides* **15**, 1401–1414.
- Nairn, J.A. 2003. Material point method calculations with explicit cracks. *Computer Modeling in Engineering and Sciences* **6**, 649–664.
- Remmerswaal, G., Vardon, P.J., Hicks, M.A. 2021. Evaluating residual dyke resistance using the Random Material Point Method. *Computers and Geotechnics* **133**, 104034.
- Sulsky, D., Chen, Z., Schreyer, H.L. 1994. A particle method for history-dependent materials. *Computer Methods in Applied Mechanics and Engineering* **118**, 179–196.
- Wu, X.Z. 2015. Modelling dependence structures of soil shear strength data with bivariate copulas and applications to geotechnical reliability analysis. *Soils and Foundations* **55(5)**, 1243–1258.
- Yin, Y., Li, B., Wang, W., Zhan, L. 2016. Mechanism of the December 2015 Catastrophic Landslide at the Shenzhen Landfill and Controlling Geotechnical Risks of Urbanization. *Engineering* **2**, 230–49.
- Zhang, X., Chen, Z., Liu, Y. 2016. *The Material Point Method: A continuum-based particle method for extreme loading cases*. Academic Press, FL, United States.
- Zhu, H., Zhang, L.M., Xiao, T. 2019. Evaluating stability of anisotropically deposited soil slopes. *Canadian Geotechnical Journal* **56(5)**, 753–760.